Models for molecular motions within polymer chains. Part 1.
A solid-state NMR study of hexane-1,6-diyl bis(p-nitrobenzoate)

Jukka P. Kujanpää and Frank G. Riddell*

School of Chemistry, The University of St Andrews, St Andrews, Scotland, UK KY16 9ST

Solid-state NMR experiments on hexane-1,6-diyl bis(p-nitrobenzoate) and its 1,1,6,6- and 2,2,5,5-deuteriated derivatives present a coherent view of the molecular dynamics of the central alkyl chain. The techniques used include ^{13}C CP/MAS spectra, ^2H quadrupole echo spectra, associated with measurements of ^{13}C $T_{1\rho}$ relaxation times, ^2H and ^{13}C T_1 relaxation times and quadrupole echo reduction factors. Molecular dynamics in the central chain are dominated by librational motions at the CH_2 groups that can best be approximated by a six-site conical model. The activation energies for these librations are *ca.* 35 kJ mol^{-1}. *gauche–trans* flips in the chain can be ruled out as the origin of the effects observed.

Introduction

Our understanding of crystalline solids is largely based upon the results of X-ray diffraction studies leading to pictures of molecular structure that often give the impression of the absence of molecular motion. In principle information about molecular motion is included in the anisotropic displacement parameters but in practice it is often difficult to extract. On the other hand nuclear magnetic resonance (NMR) spectroscopy is highly sensitive to molecular motions and, appropriately applied, forms an efficient probe of these solid state motions over a very wide range of rates.[1,2]

Although molecular motions are generally slower in solids than in liquids they have an important role in determining the macroscopic properties of solid materials. For example, the mechanical properties of solid polymers are closely related to their microscopic structures and molecular motions.[3] In addition the conductivity of solid polymer electrolytes[4] and the electrical properties of conducting polymers originate from motions at the molecular level.[5] It becomes important, therefore, to gain an understanding of the nature of these motions in polymeric systems and their relative rates and activation energies.

In the past NMR studies of molecular motions in polymeric materials have been made on the polymers themselves, often appropriately labelled with ^2H. Such studies have been made on both crystalline and amorphous materials. They have, for example, been carried out on the chain motions in polyethylene using ^{13}C $T_{1\rho}$ measurements with a high spin locking field[6] and using ^2H quadrupole echo spectra of perdeuteriated low density polyethylene isothermally crystallised from the melt.[7,8] Other systems that have been studied include poly(ethylene terephthalate),[9] poly(butylene terephthalate),[10] bulk hard-segment polyurethanes,[11] nylon 66 in crystalline[12] and amorphous[13] phases, poly(vinylidene fluoride)[14] and poly(dimethylimino)-decamethylene tetrafluoroborate.[15,16] Whilst these studies have given valuable insights into the molecular motions of alkyl chains in polymeric environments they suffer from the same general problem: a lack of precise knowledge of the crystal structures involved to allow the dynamic NMR data to be interpreted in its structural context.

We decided to adopt a different, hopefully more subtle, approach. Our studies involve crystalline solids containing short alkyl chains in which the ends of the chains are more or less firmly anchored and for which exact crystallographic
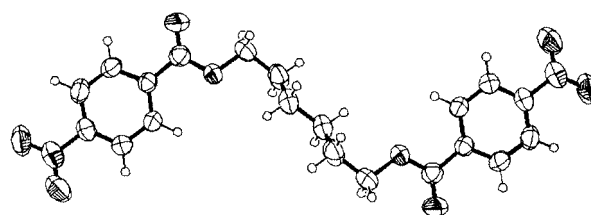

Fig. 1 Molecular structure of hexane-1,6-diyl bis(p-nitrobenzoate) as determined by single crystal X-ray diffraction.

information is available or is readily obtainable. The known conformation of the alkyl chain in the solid state can then form the sure background to the interpretation of the dynamic NMR results. These studies should be considered as following from our earlier studies of molecular motions in crystalline solids using CP/MAS techniques.[17–21]

In very general terms there are two types of chain that we should be concerned with: those in which the consecutive C–C bonds are arranged all *trans* and those in which there are some bonds that are *gauche*. For examples of the first category we examined the straight chain dicarboxylic acids in the series succinic to suberic acid. For examples of the second category we chose to examine a series of diesters made from straight chain α,ω-diols.[22] In this paper we report our studies of one of these diol derivatives, hexane-1,6-diyl bis(p-nitrobenzoate).

hexane-1,6-diyl
bis(p-nitrobenzoate)
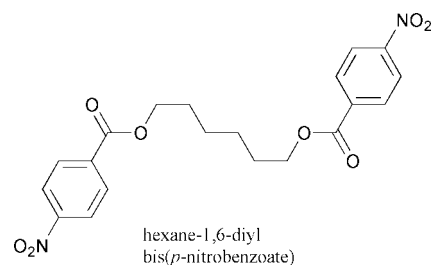
Results and discussion

Hexane-1,6-diyl bis(p-nitrobenzoate) (**1**) and its deuteriated derivatives were prepared from the appropriate hexane-1,6-diol and p-nitrobenzoyl chloride and recrystallised from an ethyl acetate–ethanol mixture. The solid state structure as derived from a single crystal X-ray diffraction study is shown in Fig. 1.
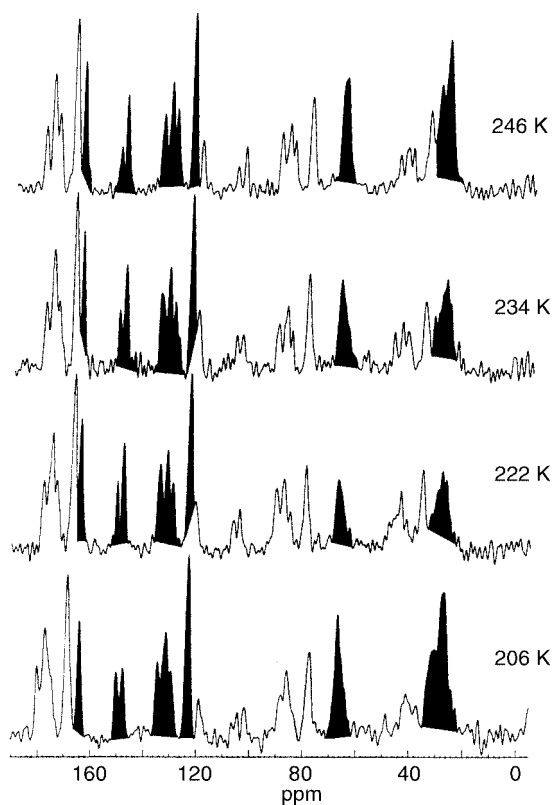
Fig. 2 ^{13}C CP/MAS spectra of hexane-1,6-diyl bis(*p*-nitrobenzoate) at various temperatures. The centre bands are shown shaded; all other spectral items are spinning side bands.

The molecule has a centre of symmetry between carbons 3 and 4 in the chain. The bonds between the carbons at positions 1 and 2 and also 5 and 6 in the chain are in a *gauche* arrangement. The other C–C bonds have *trans* arrangements. The anisotropic displacement parameters for the chain carbons are typical of those observed in small organic molecules failing to indicate any large scale molecular motion in the chain. Therefore, *trans–gauche* isomerisation is an unlikely mode of motion in this molecule, and this is later shown to be the case.

Fig. 2 shows the ^{13}C CP/MAS spectra of **1** at different temperatures. A short contact time (200 μs) was employed to maximise the intensities of the CH_2 carbons relative to the aromatic carbons. The high temperature spectra are very similar to the room temperature spectra, showing no indications of dynamic effects. However, below room temperature some interesting changes are observed. As the temperature is lowered the peaks for the chain carbons become broader and less intense than at room temperature. At 234 K their intensity is approximately 20% of their intensity at room temperature. Maximum broadening and loss of intensity are observed at around 222 K. After lowering the temperature further to 206 K some sharpening and an increase in signal intensity are observed.

The effects observed in the ^{13}C CP/MAS spectra are those of dynamic dipolar broadening which arises when the rate of the molecular motion is at or close to the precessional frequency of the protons in the decoupling field.[23] The incoherent molecular motion interferes with and makes less efficient the decoupling provided by the coherent decoupling field. In these spectra the decoupling field had a frequency of 63 kHz indicating that the frequency of the motion inside the chain is around 63 kHz at 222 K. In addition, because the decoupling field was the same as the cross polarisation field, the [13]C $T_{1\rho}$ minimum, which also causes loss of signal intensity, should occur near 222 K.

[13]C $T_{1\rho}$ relaxation times were measured for the chain carbons at different temperatures using the same spin locking field (63

Table 1 [13]C $T_{1\rho}$ relaxation times (ms) for the chain carbons of hexane-1,6-diyl bis(*p*-nitrobenzoate)

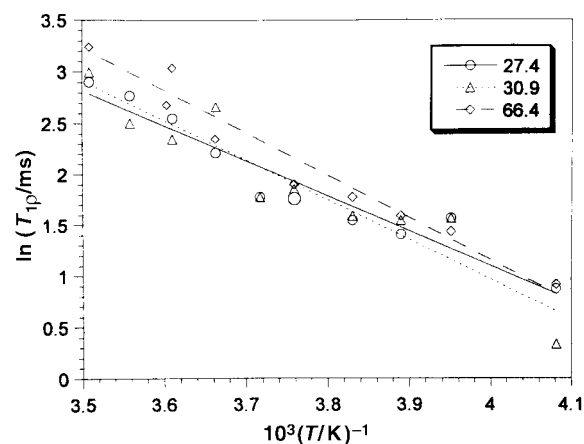| T/K	27.4 ppm	30.9 ppm	66.4 ppm
285	18.2	20.0	25.6
281	15.8	12.2	—
277	12.7	10.4	20.8
273	9.1	14.3	10.4
269	5.9	5.9	11.5
266	5.8	6.4	6.7
261	4.7	4.9	5.9
257	4.1	4.7	4.9
253	4.8	4.8	4.2
245	2.4	1.4	2.5

Fig. 3 Arrhenius plot of ^{13}C CP/MAS spectral data, $\ln(T_{1\rho})$ *vs.* $(1/T)$ for hexane-1,6-diyl bis(*p*-nitrobenzoate).

kHz) and are presented in Table 1. A recycle delay of 10 s was used at room temperature. However for this compound T_1 for ^{1}H increases with decreasing temperature, necessitating increases in the recycle delay as the temperature was lowered. This made collection of [13]C $T_{1\rho}$ data prohibitively slow below 230 K. Failure to observe the minimum in the [13]C $T_{1\rho}$ data precludes the measurement of the [13]C–[1]H dipolar interaction B^2 and therefore the rate constants for the molecular motions.[17] However, it is apparent that the minimum in the [13]C $T_{1\rho}$ data is below 230 K as predicted. Plots of $\ln(T_{1\rho})$ *vs.* $(1/T)$ give the Arrhenius activation energy (Fig. 3). The scattering of points in the plots is due to the poor signal to noise ratio. Derived activation energies are 30 kJ mol^{-1} (C 1,6) and 34 kJ mol^{-1} (C 2,5 and C 3,4). In principle, values of the [13]C–[1]H dipolar interaction B^2 can be interpreted in terms of particular modes of motion.[21] In the absence of this information the [13]C $T_{1\rho}$ data provide no indication of the mode of the motion although they provide an estimate of the energy of activation. To obtain information on the motions involved other NMR methods must be applied.

[13]C T_1 values were obtained at 358 K using the cross polarisation inversion recovery method described by Torchia.[24] After inversion the magnetisation was allowed to evolve during different time periods during which ^{1}H decoupling was accomplished by a train of saturating 90° pulses to decouple the ^{1}H resonance without introducing any nOe effects.[25] Fig. 4 shows some typical inversion recovery spectra. The recovery in the ^{13}C magnetisation was adequately described by a single exponential function from which the [13]C T_1 values were obtained. These were found to be 490 ± 35 ms for C(1,6), 245 ± 14 ms for C(2,5) and 270 ± 16 ms for C(3,4). The central carbons in the chain C(2,3,4,5) are relaxing about twice as fast as the end carbons, indicating that they are moving more slowly than C(1,6). In principle this agrees with the higher activation energy found for the central carbons. Interestingly, over the period in which the aliphatic carbons relax completely, the aromatic carbons show virtually no relaxation indicating that the *p*-nitrophenyl groups
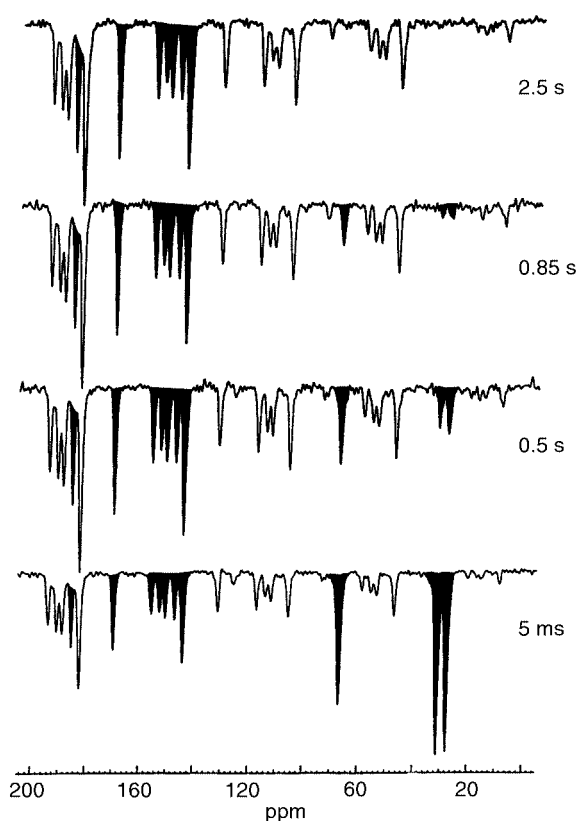
Fig. 4 Typical ^{13}C CP/MAS inversion recovery spectra for hexane-1,6-diyl bis(p-nitrobenzoate). The centre bands are shown shaded; all other spectral items are spinning side bands.

can be regarded as essentially static compared with the aliphatic chain.

Two different ^{2}H labelled samples were prepared for ^{2}H NMR studies. The alkyl chain was deuteriated either in the 1,6 positions or in the 2,5 positions yielding respectively 1,1,6,6-d$_4$-hexane-1,6-diyl bis(p-nitrobenzoate) and 2,2,5,5-d$_4$-hexane-1,6-diyl bis(p-nitrobenzoate). ^{2}H spin lattice relaxation times were measured for both samples over a variety of temperatures. The results are recorded in Table 2 and plotted as $\ln(T_1)$ *versus* $(1/T)$ in Fig. 5.

For both samples the ^{2}H spin lattice relaxation times decrease strongly with increasing temperature until a minimum occurs at *ca.* 350 K. The logarithmic plot (Fig. 5) is satisfactorily linear between *ca.* 290 and 200 K. Least squares fits in this region give lines from which activation energies of 35 and 36 kJ mol^{-1} can be derived for the 1,1,6,6-d$_4$ and the 2,2,5,5-d$_4$ derivatives respectively. These activation energies are satisfyingly in agreement with the values of 34 kJ mol^{-1} obtained from the ^{13}C $T_{1\rho}$ values.

It is now of interest to estimate the temperature of the ^{13}C $T_{1\rho}$ minimum from the ^{2}H T_1 relaxation time data. The correlation time is 1.2×10^{-9} s at the ^{2}H T_1 minimum where $\omega_o \tau_c = 0.6$ while it is only 2.5×10^{-6} s at the ^{13}C $T_{1\rho}$ minimum where $\omega_1 \tau_c = 1.0$. Using these values and an activation energy of 35 kJ mol^{-1} in the Arrhenius equation gives a value of *ca.* 210 K for the position of the ^{13}C $T_{1\rho}$ minimum. This falls nicely in line with both the ^{13}C $T_{1\rho}$ data and the temperature of maximum dipolar broadening (*ca.* 220 K).

^{2}H quadrupole echo spectra were obtained at different temperatures using 20 and 160 µs refocusing delays. Spectra for the 1,1,6,6-d$_4$ derivative are shown in Fig. 6. Above 290 K the lineshape is independent of the length of the refocusing delay, indicating that the frequency of the molecular motion is in the fast exchange limit. However, below 290 K the intensity of the central area of the spectra decreases with increasing refocusing delay, suggesting that the exchange is in the intermediate rate

Table 2 ^{2}H spin-lattice relaxation times for 1,1,6,6-d$_4$-hexane-1,6-diyl and 2,2,5,5-d$_4$-hexane-1,6-diyl bis(p-nitrobenzoates)

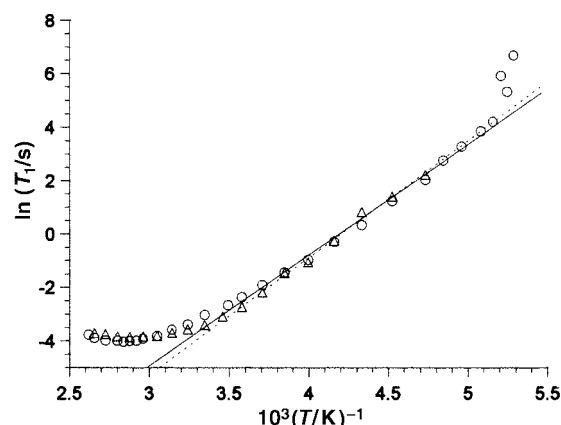| T/K	1,1,6,6-d$_4$	2,2,5,5-d$_4$
189	812	—
190	209	—
191	381	—
194	68.0	—
197	48.0	—
202	27.0	12.9
206	16.0	—
211	7.70	9.3
221	3.50	4.1
231	1.41	2.3
241	0.752	0.772
250	0.384	0.351
260	0.240	0.236
270	0.149	0.111
279	0.0940	0.0650
286	0.0700	—
289	—	0.0457
299	0.0480	0.0333
309	0.0340	0.0284
318	0.0280	0.0250
328	0.0220	0.0222
338	0.0203	0.0217
343	0.0186	—
347	0.0182	0.0213
352	0.0178	—
357	0.0186	0.0217
367	0.0188	0.0236
377	0.0204	0.0247
381	0.0232	—

Fig. 5 Arrhenius plot of ^{2}H T_1 data *vs.* $(1/T)$ for 1,1,6,6-d$_4$-hexane-1,6-diyl (○) and 2,2,5,5-d$_4$-hexane-1,6-diyl (△) bis(p-nitrobenzoates).

region, *i.e.* less than 10^7 Hz. This is consistent with the observation of the dipolar broadening in the ^{13}C CP/MAS spectra and the short ^{13}C $T_{1\rho}$ relaxation times below 270 K. At 357 K an apparent third inflection point is observed in the line shape, suggesting that the molecular motion induces asymmetry in the spectrum. A spectrum obtained at 367 K (Fig. 7), however, indicates that the spectrum is actually a superposition of two slightly different spectra.

The ^{2}H quadrupole echo spectra for both labelling patterns were best simulated with the six-site conical libration model (see Appendix 1) using the parameters given in Table 3 although a two-site exchange model produced suitable lineshapes for the 1,1,6,6-d$_4$ derivative. The spectra obtained at 357 K and above were simulated using two distributions. Interestingly only a small change in the standard deviation of the distribution broadens the spectrum so that the splitting clearly visible in the spectrum measured at 367 K is invisible in the spectra at 357 and 377 K.

Quadrupole echo spectra for the 2,2,5,5-d$_4$ derivative are shown in Fig. 8. At 211 and 231 K power patterns of width 114
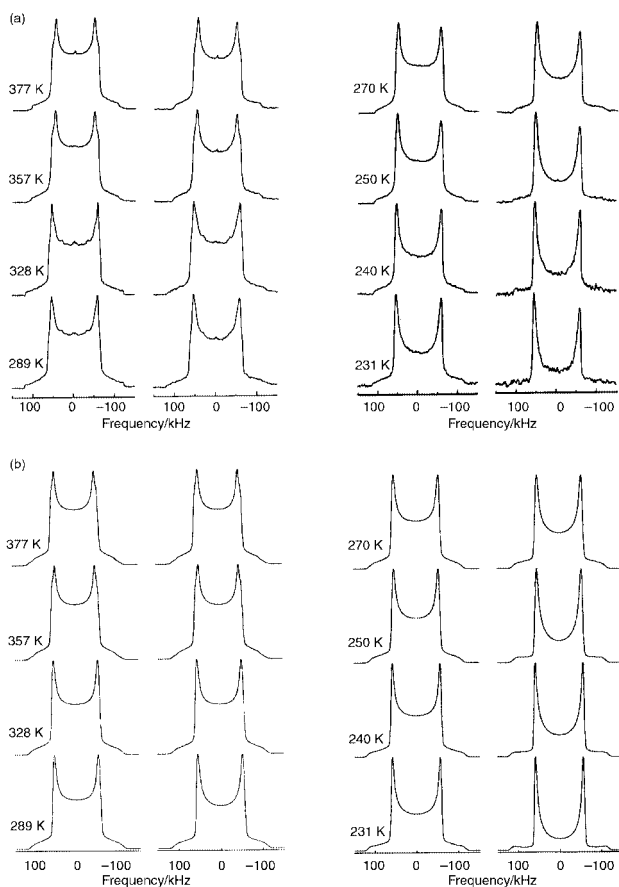
Fig. 6 Observed (a) and calculated (b) quadrupole echo spectra for 1,1,6,6-d$_4$-hexane-1,6-diyl bis(*p*-nitrobenzoate) at varying temperatures.
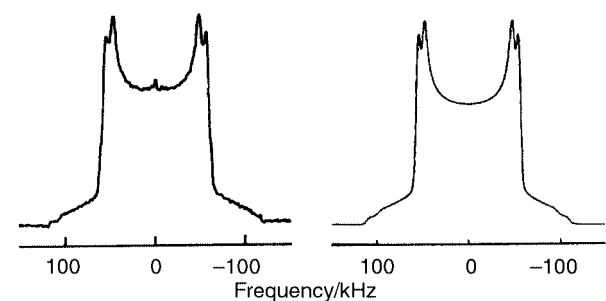

Fig. 7 Observed (left) and calculated (right) quadrupole echo spectra for 1,1,6,6-d$_4$-hexane-1,6-diyl bis(*p*-nitrobenzoate) at 367 K.

and 133 kHz were observed respectively. At these temperatures the intensity in the central portion of the spectrum drops with an increase in the refocusing delay, indicating that the rate of the librational motion is in the intermediate rate range in keeping with the ^{13}C CP/MAS spectra and the ^{13}C $T_{1\rho}$ data. At 250 K the central region of the spectrum with the 20 µs delay is dome-shaped while only a small hump is observed in the spectrum with the 160 µs delay. The dome of the 20 µs delay spectrum sharpens at 270 K whilst the 160 µs delay spectrum becomes dome-like at this temperature. At 279 K the spectra at both refocusing delays are very similar, indicating that the rate of motion is almost in the fast motion limit, *i.e.* the rate of motion is *ca.* 10^7 s^{-1} and the central dome has sharpened into a peak at zero frequency. At higher temperatures the proportion of this peak increases and the proportion of the remaining powder pattern decreases, indicating that the motion increasingly mimics isotropic motion.

The ^{2}H quadrupole echo spectra were best simulated by the six-site conical libration model (Appendix 1) with the param-
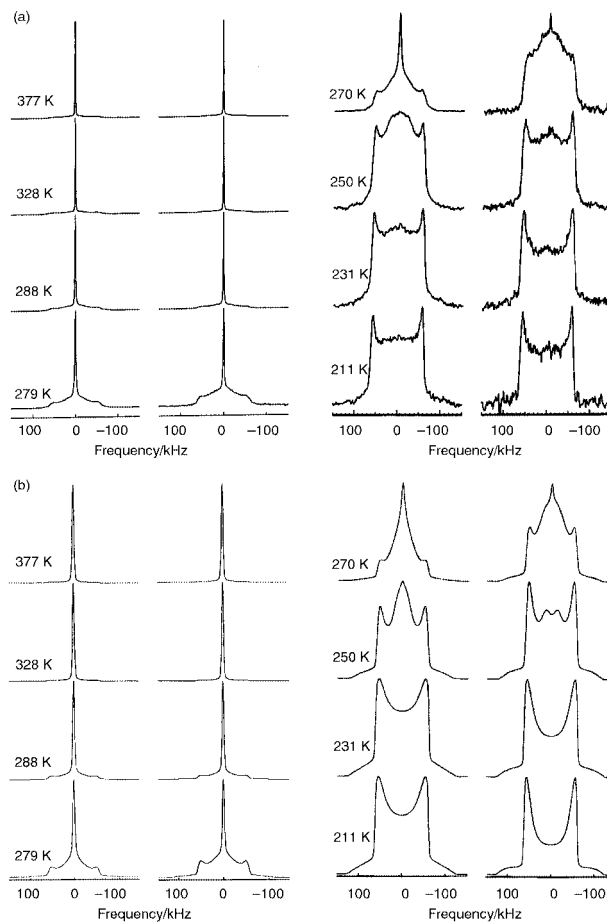
Fig. 8 Observed (a) and calculated (b) quadrupole echo spectra for 2,2,5,5-d$_4$-hexane-1,6-diyl bis(*p*-nitrobenzoate) at varying temperatures.

eters given in Table 3. The simulated spectra are shown in Fig. 8. As for the 1,1,6,6-d$_4$ derivative the simulation is difficult because the rate and amplitude of the motion change simultaneously. Also, the six-site conical libration model, although the best available, is only a very crude model for the actual libration of the C–D bonds in the chain. Refinement of the model would be difficult and probably require more powerful computing resources. Nevertheless, the simple six-site conical libration model satisfactorily reproduces the observed spectra.

The simulation also produces another significant result. For our conical libration model the dome first appears in the 20 µs spectrum and then in the 160 µs spectrum as is observed experimentally with increasing temperature. For a *trans–gauche* exchange the simulation produces this change in the opposite sense. *trans–gauche* exchange is, therefore, excluded by this result.

A final NMR test that can be applied to the deuteriated model compounds is measurement of the echo reduction factor against temperature as shown in Fig. 9 (Appendix 2). The echo reduction factor is defined as the ratio of the height of the echo using a refocusing delay of 160 µs compared to that at 20 µs. For the 1,1,6,6-d$_4$ derivative the echo reduction factor increases from 0.3 at 220 K to a plateau of 0.5 at temperatures above 300 K. This indicates that the rate of the librational motion increases during this temperature region from the intermediate exchange region to the fast motion limit. For the 2,2,5,5-d$_4$ derivative the dependence of the echo reduction factor on temperature is similar although not quite as smooth as for its isomer. It increases from 0.35 at 210 K to 0.75 at 375 K. The larger value of 0.75 suggests that the dipolar coupling weakens at high temperatures in keeping with the observation of the isotropic peak in the quadrupole echo spectra.

Table 3 Parameters for simulation of quadrupole spectra

Spectrum	k/s^{-1}	p	θ_0	$\Delta\theta$	W_{calc}/kHz	W_{obs}/kHz
1,1,6,6-d$_4$						
377 K outer	1×10^8	80	15	3	—	—
inner		100	22	1	96	94
367 K outer	1×10^8	100	15	1	108	111
inner		50	22	1	96	95
357 K outer	1×10^8	80	15	3	—	—
inner		100	22	1	96	96
328 K	1×10^8	100	15	3	107	112
289 K	1×10^7	100	15	3	107	112
270 K	5×10^6	100	15	3	107	106
250 K	2×10^6	100	15	3	107	108
240 K	1×10^6	100	10	3	114	115
231 K	5×10^5	100	10	3	114	115
2,2,5,5-d$_4$						
377 K outer	1×10^8	2	15	5	—	—
inner		1	45	10	—	—
peak		100	55	1	—	—
328 K outer	1×10^8	2	15	5	—	—
inner		1	45	10	—	—
peak		100	55	1	—	—
288 K outer	1×10^8	10	15	5	—	—
inner		5	45	10	—	—
peak		100	55	1	—	—
279 K outer	1×10^7	30	15	5	—	—
inner		15	45	10	—	—
peak		100	55	1	—	—
270 K outer	5×10^6	100	15	5	108	104
inner		100	45	5	—	—
250 K outer	5×10^6	100	15	5	108	108
inner		30	45	5	—	—
231 K	2×10^6	100	10	10	108	113
211 K	1×10^6	100	10	10	108	114
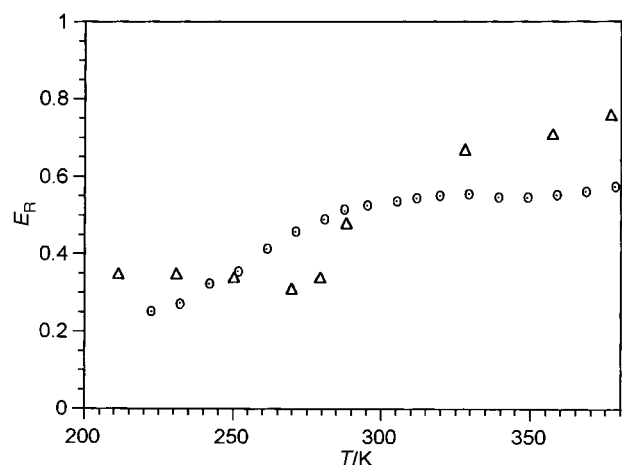
Fig. 9 Echo reduction factor as a function of temperature for 1,1,6,6-d$_4$-hexane-1,6-diyl (○) and 2,2,5,5-d$_4$-hexane-1,6-diyl (△) bis(p-nitrobenzoates).

Experimental

NMR spectroscopy

All solid-state NMR spectra were obtained on a Bruker MSL500 spectrometer operating at 500.13 MHz for ^{1}H, 125.758 MHz for ^{13}C and 76.773 MHz for [2]H. [13]C CP/MAS spectra were obtained using a Bruker double tuned probe with 4 mm zirconia rotors spinning at *ca.* 6 kHz. A standard cross polarisation sequence was used for most spectra. [13]C T_1 relaxation times were measured with a modified ^{13}C CP/MAS inversion recovery sequence derived from that described by Torchia.[24] The continuous wave ^{1}H decoupling sequence of Torchia was

replaced by a train of saturating 90° pulses as described by Gabrys *et al.*[25] Temperatures were calibrated as described previously by us.[26]

[2]H spectra were obtained using a 5 mm single tuned Doty probe with sapphire rotors that were prevented from spinning by insertion of a small wedge of paper. For the ^{2}H spectra the 90° pulse width was determined using the multipulse tune-up sequence of Gernstein.[27] The standard quadrupole echo pulse sequence 90°$_{\pm x}$–τ_1–90°$_{\pm x}$–τ_2–acq was used with a 90° pulse of *ca.* 3.8–3.9 μs, τ_1 20 or 160 μs and τ_2 shorter than τ_1 so that the echo top was clearly visible. The spectral width employed was 2.5 MHz and the FID was collected in between 1 k and 3 k data points and transformed in 8 k data points after a line broadening of 1 kHz had been applied. An appropriate recycle delay between 200 ms and 100 s was used depending on the ^{2}H relaxation time. Free induction decays were left shifted to the echo maximum before Fourier transformation. [2]H relaxation times were measured with a saturation recovery method using a quadrupole echo detection similar to that of Hirschinger *et al.*[12] The pulse sequence was [90°–τ_0]$_n$90°–vd–90°–τ_1–90°–τ_2–acq where the delay τ_0 was 3 ms and the delay vd was varied from 1 ms to 100 s as appropriate. τ_1 was 20 μs and τ_2 was shorter than τ_1 so that the top of the echo was visible. Temperatures in this probe were calibrated using [27]Al spin-lattice relaxation times across the whole temperature range.[28,29]

Quadrupole echo spectra were calculated using the program MXET1 of Greenfield *et al.*[30] compiled onto a Sun Sparcstation 4 workstation.

X-Ray crystallography

Data were collected on a Rigaku AFC7S diffractometer using

Table 4 Crystallographic data for hexane-1,6-diyl bis(*p*-nitro-benzoate)

Empirical formula	$C_{20}H_{20}N_2O_8$
Formula weight	416.39
Crystal colour, habit	Colourless, block
Crystal system	Monoclinic
Lattice type	Primitive
Lattice parameters	$a = 8.982(3)$ Å
	$b = 12.471(3)$ Å
	$c = 9.086(3)$ Å
	$\beta = 92.91(3)°$
	$V = 1016.4(5)$ Å³
Space group	$P2_1/n$
Z	2
D_{calc}/g cm⁻³	1.360
F_{000}	436.00
μ(Mo-Kα)/cm⁻¹	1.06

Mo-Kα radiation. The structure was solved by direct methods and refined by a full matrix least-squares procedure. Crystallographic data are given in Table 4.†

Synthesis

Hexane-1,6-diyl bis(*p*-nitrobenzoate) samples were prepared from the appropriate hexanediol by reaction with *p*-nitrobenzoyl chloride in the presence of two equivalents of pyridine and were recrystallised from mixed ethanol–ethyl acetate. Sample melting points were all in the range 120–122 °C (lit. mp 120 °C).[31] Crystals for single crystal X-ray diffraction were obtained by slow evaporation from a solution in CH_2Cl_2–acetone (1:1).

2,2,5,5-d₄-adipic acid was obtained from disodium adipate using the method of Atkinson *et al.*[32] Disodium adipate (25 mmol) was dissolved in D_2O (10 cm³) containing OD⁻ (2.5 mmol) and heated in an autoclave at 150 °C for 24 hours. This process was repeated until the isotopic content was over 90%.

Tetradeuteriated hexane-1,6-diol was obtained from the appropriate adipic acid sample by conversion to the methyl ester, *via* the acid chloride, which was then reduced either with lithium aluminium hydride or lithium aluminium deuteride under standard conditions in anhydrous diethyl ether. Typically 5 g of adipic acid yielded 3.39 g (83%) of solid hexanediol.

Conclusions

The results of the NMR experiments described above that we have carried out on hexane-1,6-diyl bis(*p*-nitrobenzoate) and its deuteriated derivatives present a coherent view of the molecular dynamics of the central alkyl chain. Dynamic NMR techniques including ¹³C CP/MAS spectra, ²H quadrupole echo spectra, associated with measurements of ¹³C $T_{1\rho}$ relaxation times, ²H and ¹³C $T_{1\rho}$ relaxation times and quadrupolar echo reduction factors produce a coherent, satisfying and very satisfactory picture of molecular motion in this model of a section of a polymer chain. Molecular dynamics in this chain are dominated by librational motions at C(1,6) and C(2,5) in the central chain that can be best and satifactorily approximated by a six-site conical model. The activation energies for these librations are *ca.* 35 kJ mol⁻¹. The *p*-nitrobenzoate groups are essentially static on the time scale for molecular motions of the alkyl chains.
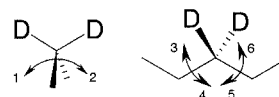
Fig. 10 Model used to describe the six-site conical libration model.

Appendix 1 Models for molecular motion

Various models have been proposed for the librational modes of CH_2 groups in alkyl chains. The simplest is two-site exchange which simply involves a C–D bond exchanging between two different orientations. Three-site conical motion involves three orientations for the C–D bond of which the simplest example is a methyl group rotation. Conical exchange does not necessarily imply three sites and we have employed a six-site conical model (*vide infra*). Exchange between four tetrahedrally located sites is often termed exchange in the diamond lattice and has been widely used to describe molecular motions of polymers in solution.[33] In solids, however, the full four-site exchange involves large displacements of the polymer tail and therefore is more likely in the amorphous phase than in the crystalline phase. Three-site exchange in the diamond lattice describes *gauche–trans* exchange about one carbon–carbon bond.

For the compounds we have been studying, a six-site conical motion model has given the best correspondence between experimental and calculated spectra and is preferred over the two- or three-site models. It can be visualised as arising from libration of the chain about its long axis to give two of the sites and from simultaneous rotation of the two C–C bonds in both directions giving the four other sites (Fig. 10). Although the six sites produced with the rotations described in Fig. 10 are not equally spaced, this random librational motion may be visualised as a motion in a six-site cone with a half angle β and with all the sites 60° apart to facilitate computation. Failure to simplify in this way would make the resulting calculations of line shapes extremely complex and this is the model used in this paper.

The conical libration model proposed by Hirschinger *et al.* in their simulation of the line shapes for selectively deuteriated nylon 66 polymer[12] does not give a good fit to the data in this paper. Their conical libration model assumes that the C–D bond is librating over a wide range of angles and that this librational motion is described well by a harmonic oscillator in its 11 lowest energy levels. Therefore, the probability distribution for the librational angles is approximated by a Gaussian density function. This model fails to explain the results in this paper since it requires very large displacements for the atoms in the chain to produce the dome-like spectra we observe which is contrary to the X-ray diffraction anisotropic displacement parameter results. It also fails to reproduce the relatively sharp isotropic peak in the centre of the spectrum.

Miura *et al.*[13] used a different model for deuteriated amorphous nylon 66 for which a sharp peak in the centre of the spectrum was observed. This model consisted of three different component spectra that were summed in different ratios to produce the observed spectra. The components represented different segments of the chain undergoing exchange at different rates. The sharp central peak arose from segments undergoing rapid anisotropic motion. Since there are no regions in the chains of our crystalline materials where fast anisotropic motion can occur the model of Miura *et al.* is inappropriate for our compounds.

Appendix 2 Echo reduction factor

The theoretical basis of the quadrupole echo reduction factor is well known,[34–37] but it has not been widely applied due to

experimental difficulties in its observation. These include the wide temperature range needed to understand the result properly, the good S/N ratio needed to avoid losing the signal completely for longer delays, the reduction due to D–H dipolar coupling in organic molecules, and the experimental difficulties in quadrupole echo measurement itself. There follows a brief description of the application of the technique. For the theory the reader is referred to the references cited above. For further information the reader is referred to the PhD thesis of one of the authors (JPK).[38]

When measuring ^2H quadrupole echo spectra to differentiate between different models for molecular motion it is important that spectra are measured with different refocusing delays (τ_1) and that these spectra are compared with the simulated spectra. The measurement of quadrupole echo spectra in the intermediate exchange regime is, however, very time consuming for long refocusing delays since the echo intensity decays exponentially with the refocusing delay. In addition to the motional effects (T_2) in the intermediate exchange region the echo intensity is also decreased by dipolar couplings between deuterons and protons as the quadrupole echo sequence fails to refocus these couplings. Dipolar couplings also broaden the line shape and their effect can be taken into account by multiplying the free induction decay by a Gaussian broadening function that is a few kilohertz wide. Such a broadening has a fairly small effect on the line shape but the decrease in the echo intensity during the refocusing delay is considerable. Choosing refocusing delays of 20 and 160 μs and an effective 2 kHz broadening it can be shown that the effect is an echo reduction of 0.67, and for an effective 3 kHz broadening the corresponding reduction would be 0.40. Thus dipolar couplings reduce the echo intensity to about half its original intensity in addition to the T_2 effects in the intermediate exchange region. Thus for our chosen delays of 20 and 160 μs we expect an echo reduction factor of *ca.* 0.5. If the echo reduction factor falls below this it is indicative of T_2 effects becoming important during the refocusing delay (see Fig. 9). If the echo reduction factor is greater than this it seems likely that the dipolar couplings between deuterons and protons are becoming less important.

References

1 K. D. M. Harris and A. E. Aliev, *Chem. Br.*, 1995, **31**, 132.
2 C. L. Perrin and T. J. Dwyer, *Chem. Rev.*, 1990, **90**, 935.
3 B. F. Chmelka and A. Pines, *Science*, 1989, **246**, 71.
4 F. M. Gray, *Solid Polymer Electrolytes*, VCH Publishers, New York, 1991.
5 A. R. Blythe, *Electrical Properties of Polymers*, Cambridge University Press, Cambridge, 1979.
6 D. L. VanderHart and A. N. Garroway, *J. Chem. Phys.*, 1979, **71**, 2773.
7 H. W. Spiess, *Colloid Polym. Sci.*, 1983, **261**, 193.
8 D. Hentschel, H. Sillescu and H. W. Spiess, *Polymer*, 1984, **25**, 1078.
9 M. D. Sefcik, J. Schaefer, O. E. Stejskal and R. A. Mackay, *Macromolecules*, 1980, **13**, 1132.
10 L. W. Jelinski, J. J. Dumais and A. K. Engel, *Macromolecules*, 1983, **16**, 492.
11 A. Kitanar and L. W. Jelinski, *Macromolecules*, 1986, **19**, 1876.
12 J. Hirschinger, H. Miura, K. H. Gardner and A. D. English, *Macromolecules*, 1990, **23**, 2153.
13 H. Miura, J. Hirschinger and A. D. English, *Macromolecules*, 1990, **23**, 2169.
14 J. Hirschinger, D. Schaefer, H. W. Spiess and A. J. Lovinger, *Macromolecules*, 1991, **24**, 2428.
15 D. Schaefer, R. R. Rietz, W. H. Meyer and H. W. Spiess, *Ber. Bunsenges. Phys. Chem.*, 1991, **95**, 1071.
16 R. R. Rietz, D. Schaefer, W. H. Meyer and H. W. Spiess, *Electrochim. Acta*, 1992, **37**, 1657.
17 F. G. Riddell, S. Arumugam, K. D. M. Harris, M. Rogerson and J. H. Strange, *J. Am. Chem. Soc.*, 1993, **115**, 1881.
18 F. G. Riddell, G. Bernáth and F. Fülöp, *J. Am. Chem. Soc.*, 1995, **117**, 2327.
19 F. G. Riddell and M. Rogerson, *J. Chem. Soc., Perkin Trans. 2*, 1996, 493.
20 F. G. Riddell and M. Rogerson, *J. Chem. Soc., Perkin Trans. 2*, 1997, 249.
21 F. G. Riddell, K. S. Cameron, S. A. Holmes and J. H. Strange, *J. Am. Chem. Soc.*, 1997, **119**, 7555.
22 For a discussion, see J. Kujanpää, PhD thesis, University of St Andrews, 1999.
23 W. P. Rothwell and J. S. Waugh, *J. Chem. Phys.*, 1981, **74**, 2721.
24 D. A. Torchia, *J. Magn. Reson.*, 1978, **30**, 613.
25 B. Gabrys, H. Fumitaka and R. Kitamaru, *Macromolecules*, 1987, **20**, 175.
26 F. G. Riddell, R. A. Spark and G. V. Günther, *Magn. Reson. Chem.*, 1996, **34**, 824.
27 B. C. Gernstein, *Philos. Trans. R. Soc. London, A*, 1981, **299**, 521.
28 K. Müller, P. Meier and G. Kothe, *Prog. Nucl. Magn. Reson. Spectrosc.*, 1985, **17**, 211.
29 D. P. Tunstall, personal communication.
30 M. S. Greenfield, A. D. Ronemus, R. L. Vold, R. R. Vold, P. D. Ellis and T. E. Raidy, *J. Magn. Reson.*, 1987, **72**, 89.
31 K. Heyns and O. F. Woyrsch, *Chem. Ber.*, 1953, **86**, 76.
32 J. G. Atkinson, J. J. Csakvary, G. T. Herbert and R. S. Stuart, *J. Am. Chem. Soc.*, 1968, **90**, 498.
33 F. Heatley, *Prog. Nucl. Magn. Reson. Spectrosc.*, 1979, **13**, 47.
34 A. Abragam, *The Principles of Nuclear Magnetism*, Oxford University Press, Oxford, 1961.
35 H. W. Spiess and H Sillescu, *J. Magn. Reson.*, 1981, **42**, 381.
36 R. J. Schadt, E. J. Cain and A. D. English, *J. Phys. Chem.*, 1993, **97**, 8387.
37 T. -H. Lin and R. R. Vold, *J. Magn. Reson., Ser. A*, 1995, **113**, 271.
38 J. P. Kujanpää, PhD thesis, St Andrews, 1999.